



Segregation of respirable dust for chemical and toxicological analyses

Teresa L. Barone, Taekhee Lee, Emanuele G. Cauda, Andrew L. Mazzella, Robert Stach & Boris Mizaikoff

To cite this article: Teresa L. Barone, Taekhee Lee, Emanuele G. Cauda, Andrew L. Mazzella, Robert Stach & Boris Mizaikoff (2021) Segregation of respirable dust for chemical and toxicological analyses, Archives of Environmental & Occupational Health, 76:3, 134-144, DOI: [10.1080/19338244.2020.1779018](https://doi.org/10.1080/19338244.2020.1779018)

To link to this article: <https://doi.org/10.1080/19338244.2020.1779018>



Published online: 18 Jun 2020.



Submit your article to this journal [↗](#)



Article views: 78




View related articles [↗](#)



View Crossmark data [↗](#)



Segregation of respirable dust for chemical and toxicological analyses

Teresa L. Barone^a, Taekhee Lee^a, Emanuele G. Cauda^a, Andrew L. Mazzella^a, Robert Stach^b, and Boris Mizaikoff^b 

^aPittsburgh Mining Research Division, National Institute for Occupational Safety and Health, Centers for Disease Control and Prevention, Pittsburgh, PA, USA; ^bInstitute of Analytical and Bioanalytical Chemistry, Ulm University, Ulm, Germany

ABSTRACT

Respirable dust can pass beyond ciliated airways of the respiratory tract and influence adverse health effects. Health effects can be studied using samples generated from bulk dust segregation. Because previous segregation methods diverge from size-selection criteria of the international convention for respirable particles (ICRP), a method was developed to approximate the ICRP. The method was compared to an ideal sampler by measuring the sample collection bias. The comparison shows that the uncertainty due to the bias was 0.10 based on European Standard EN13205:2014 criteria, which indicates that the segregator effectively follows the ICRP. Respirable particle size distributions were confirmed by an aerodynamic particle sizer and by computer-controlled scanning electron microscopy. Consequently, a systematic way to generate respirable powders for health effects studies and chemical analyses was developed.

KEYWORDS

Air pollution; dust; particle size; particulate matter; sample preparation

Introduction

Exposure to respirable dust adversely affects workers' health in the construction, agriculture, and mining industries.^{1–4} Large communities are also affected due to dust storms in areas such as Arizona, U.S.⁵ Southern Israel,⁶ and Sydney, Australia.⁷ Respirable dust is a health concern because of its penetration to the lung and biologically active surface area.^{8–11} Its cumulative exposure is associated with the development of chronic obstructive pulmonary disease (COPD).^{12–13} COPD can occur with exposure to relatively low-toxicity components of respirable dust such as limestone¹⁴ and a highly toxic component—crystalline silica.¹⁵

Exposure to crystalline silica is a major cause of dust-related respiratory illnesses (Donaldson, 2012; Cook et al. 2005).^{16–17} Illnesses such as silicosis and lung cancer are associated with exposure to respirable crystalline silica (RCS).¹⁸ Mechanistic studies indicate that RCS carcinogenicity depends on the surface properties of the original source dust.^{8,19–22} Source dust properties can be investigated by collecting representative samples from ambient air. However, lengthy collection times are needed to obtain enough airborne material in the respirable size range for health effects studies. Alternatively, respirable dust samples can be

obtained by bulk dust segregation. Bulk dust can be acquired from granular source material (e.g. soils) or industrial dust collectors (e.g. cyclones leading to bag-house filters²³). Subsequently, bulk dust can be segregated by an array of methods.

Previously published segregation methods address U.S. Environmental Protection Agency size-selection criteria for PM_{2.5} ($\leq 2.5 \mu\text{m}$) and PM₁₀ ($\leq 10 \mu\text{m}$).^{24–29} Size selection of atmospheric aerosols according to PM_{2.5} and PM₁₀ generally enriches samples in chemically generated (e.g. soot) and mechanically generated (e.g. dust) aerosols, respectively. For predominantly mechanically generated aerosols in occupational environments, size-selection criteria have been established by the International Standards Organization (ISO), Comité Européen de Normalization (CEN), and the American Conference of Governmental Industrial Hygienists (ACGIH) to form the international convention for respirable particles (ICRP).^{30–32} The ICRP defines efficiencies at which particles of a given size range are sampled to assess workers' exposure to respirable dust (e.g. approximately 84% at $2.5 \mu\text{m}$, 50% at $4 \mu\text{m}$, 16% at $6 \mu\text{m}$).

Size selection of samples according to the ICRP was approximated by segregating bulk dust in liquids through sedimentation as described in a publication

on the size-weighted relevant fine fraction (SWeRF) method.³³ Dust segregation by sedimentation can be challenging due to dust agglomeration in solution (i.e. coagulation, flocculation). Often surfactants or dispersants are required to deagglomerate dust in liquid suspensions, and those dispersants can alter sample properties and introduce artifacts in health studies. For this reason, it is preferred to segregate dust using dry methods.

To the authors' knowledge, the only dry method for respirable dust segregation was developed by Liu and colleagues²⁸ for lunar dust. The authors estimated a 50% cutoff diameter ($_{50}d_{ae}$) of 3.1–3.7 μm , which is near the ICRP recommendation of 4 μm . However, measurements were not made for the $_{50}d_{ae}$, the size-dependent sampling efficiency, or the sampling bias relative to the ICRP. These were lacking because the inlet and outlet concentrations for narrow particle size ranges were not measured. Furthermore, due to the unconventional design of the segregator, the parameters could not be modeled.

Segregation according to the ICRP is advantageous because it allows for the systematic control of particle size range so that toxicity information can be compared across different studies. Also, the variation of other properties, such as chemical composition and surface activity, can be systematically tested. Furthermore, it allows the generation of surrogates for occupational respirable dust and their mixtures. The possibility to generate large quantities of respirable dust of single minerals or mixtures can lead to the preparation of calibration samples and standard material for analytical methods development and evaluation. Mixtures such as RCS in mine dust,³⁴ endotoxins in agricultural dust,³⁵ and heavy metals in construction dust³⁶ can be generated for mechanistic studies.

In the current work, a dust segregator was developed to follow the ICRP. Dust was dispersed and de-agglomerated with a powder disperser, size-separated with a sharp-cut cyclone, and amassed on a 70 mm filter. To evaluate the particle size distributions of segregated dust, measurements were made using an aerodynamic particle sizer (APS) and computer-controlled scanning electron microscope (CCSEM).

Methods

The dust segregator was configured to allow consistent size separation by a cyclone. Subsequently, the cyclone was calibrated by adjusting the flow rate and measuring the size distribution of penetrating particles. At the selected flow rate, cyclone performance

was compared to particle size-selective criteria of the ICRP, as conventionally done in an aerosol chamber. Following verification in the chamber, the cyclone was mounted in the dust segregator and respirable dust segregation was confirmed by APS (Model 3321, TSI Inc. Shoreview, MN) and CCSEM (Model Express, ASPEx, Delmont, PA) measurements.

Dust segregator development

A cyclone was adapted for respirable dust separation, interfaced with a dust disperser, and coupled to a particle filter. The primary challenge was to overcome the pressure drop across the filter and maintain the segregator flow rate as the respirable dust loading increased. The small-scale powder disperser (SSPD) (Model 3433, TSI Inc. Shoreview, MN) was selected to disperse bulk dust because it maintains integrity under pressure or vacuum conditions, which can occur when in-line with a filter. (If the filter clogs (or breaks), the disperser may experience high pressure (or vacuum)). In addition, the SSPD has the advantage that it accepts bulk dust with large particles (100 μm) and requires very little sample (< 1 g), while the commonly used fluidized bed dust generator malfunctions if large particles are present due to a clogged port and requires an appreciable sample. Also, the fluidized bed generator is unfavorable for in-line operation with a filter because it can eject bronze beads when pressurized or under vacuum.

The SSPD was modified by adding a mass flow controller (MFC) to maintain a stable flow rate of air for dust aerosolization and subsequent cyclone separation. The MFC was added to the compressed air that drove the Venturi aspirator. Another modification was the removal of sheath air at the sample inlet because of sample disturbance and the addition of high-efficiency particle arrestor (HEPA)-filtered air about a meter away from the instrument (6,000 liters per minute (lpm)) to provide particle-free background air. Lastly, rather than sampling a portion of the aerosol as in the original configuration, the total aerosol was transferred from the SSPD to the cyclone to minimize sample losses.

The cyclone was a sharp-cut prototype, custom made by BGI (Waltham, MA). It was selected because it could be operated at high flow rates to improve yield and could be thoroughly cleaned to prevent sample-to-sample contamination. The construction was stainless steel except for the O-ring which sealed the grit pot.

Dust separated by the cyclone was collected on a 70-mm filter with an effective pore size of 5 μm (Figure 1). The relatively large filter diameter and

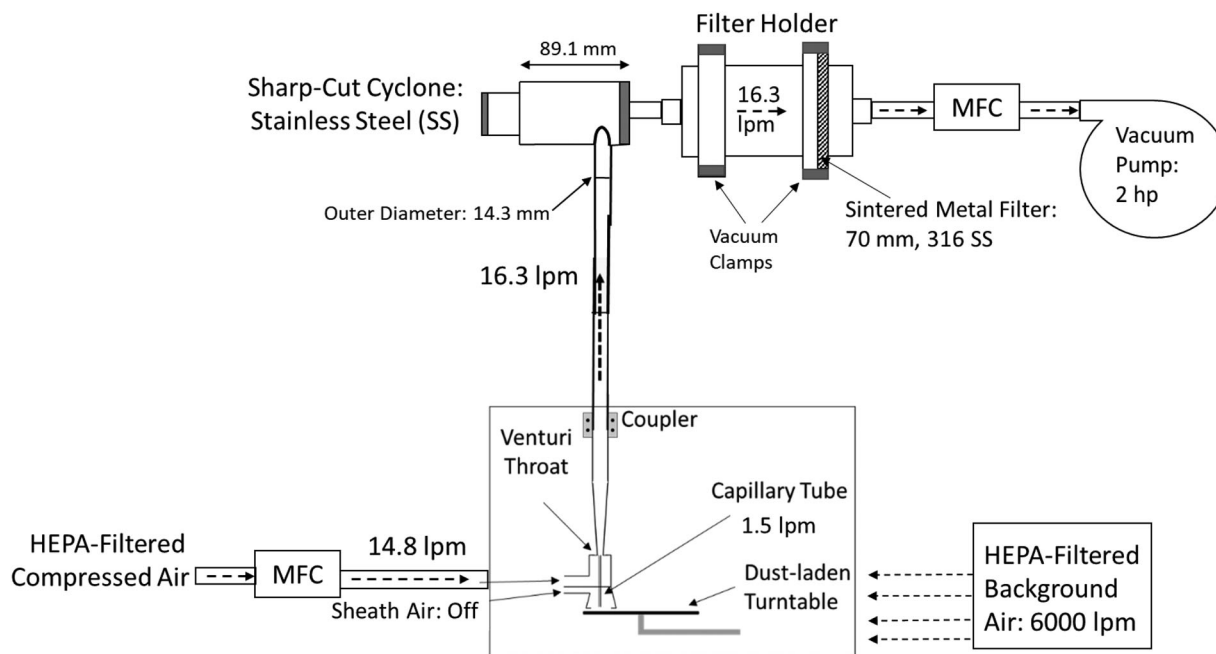


Figure 1. Sketch of respirable dust segregator.

effective pore size permitted an adequate flow rate and allowed the retention of submicron particles. A sintered-metal filter (Model 1190072-01-050, Mott Corp. CT) was used because of its durability. Despite adequate filter selection, the pressure drop across the filter became restrictive after prolonged dust collection, so a high-capacity pump of 2 horsepower (hp) (Model SOGEVAC SV40 B, Leybold USA, PA) was needed to maintain a stable flow rate for several hours of segregator operation.

The segregator was evaluated using mineral dust that could be easily dispersed (dolomite) and one that tended to cake (calcite) due to its hygroscopicity. The bulk dusts were prepared by pulverizing large crystals of calcite and dolomite (Ward's Science, NY) with an agate pestle and mortar for 5 minutes.

Cyclone flow rate selection

The cyclone was adapted for respirable dust collection through the evaluation of particle penetration for various flow rates. The evaluation was made within the segregator system by the replacement of the filter (Figure 1) with an on-line APS (Figure 2). The APS was used to measure the size distribution of particles penetrating the cyclone over a range of 0.5–20 μm with 1-second resolution. Distortion of the size distribution was prevented by matching the cyclone and APS flow velocities ($\pm 10\%$) to sample particles isokinetically.³⁷ For isokinetic sampling, the diameter of the probe leading to the APS (Figure 2) was decreased

from 7 mm to 4 mm as the cyclone flow rate was increased from 16 to 54 lpm. The probe was placed upstream of a t-fitting that allowed excess air to be purged to a HEPA filter (Figure 2). The flow rate was measured by a Gilibrator with a 2–30 lpm bubble flow cell (Sensidyne, St. Petersburg, FL) for sub-25 lpm and by a dry gas meter (Harvard Apparatus, Holliston, MA) for larger flow rates. The flow rate was varied to determine a value at which particles smaller than 4 μm passed through the cyclone and those larger were retained. The selected flow rate was evaluated for effectiveness in approximating the ICRP^{30–32} as described in the next section.

Cyclone performance comparison with the ICRP

At the selected flow rate, the cyclone was evaluated in an aerosol chamber for its characteristic penetration efficiency and ability to approximate the ICRP. The evaluation was made in an aerosol chamber, rather than the segregator system, because the chamber allows for spatially uniform and temporally stable aerosol concentrations for side-by-side measurements of the cyclone and background (pre-cyclone) concentrations. Uniform concentrations are necessary for consistent pre- and post-cyclone measurements and accurate penetration efficiency measurements. The measurement methods have been well established,^{38–40} and the current system, which includes the calm-air chamber and associated instruments was described in detail previously.⁴¹

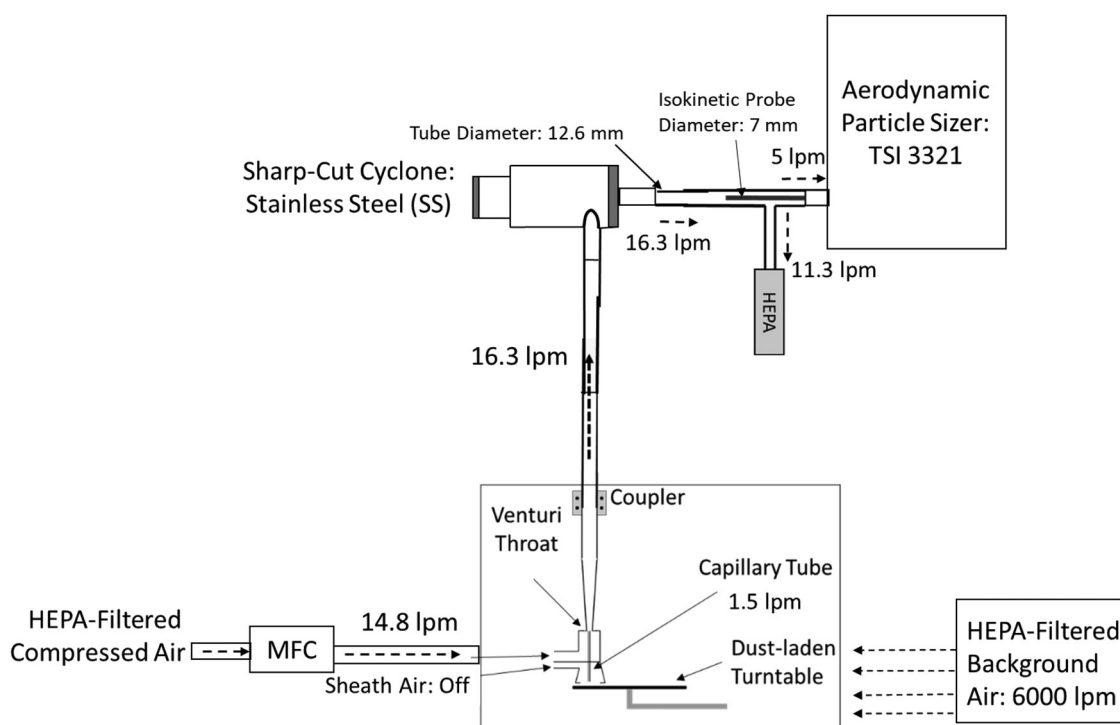


Figure 2. Sketch of segregator and isokinetic sampling system for respirable dust size distribution measurements by the aerodynamic particle sizer (APS).

Briefly, an aerosol composed of glass microspheres (Cospheric, Santa Barbara, CA) was generated at a constant rate using a fluidized bed dust generator (Model 3400 A, TSI, MN). The charge of the aerosol was neutralized by a Kr-85 source (Model 3012 A, TSI Inc. MN) before entering the calm-air chamber. The cylindrical chamber was made of fiberglass (0.45-m diameter, 2.4-m height) and was supplied with compressed, filtered air at a flow rate of 20 lpm. The generated aerosol was fed at a constant rate and was introduced at the same cross-sectional position as the filtered air to aid in adequate mixing. The calm-air conditions were maintained with a downward air velocity of 2 mm/s. To determine penetration efficiency, confirmation measurements were made to ensure a uniform aerosol concentration in the sampling zone.

Penetration efficiency was determined by dividing the post-cyclone number concentration by the pre-cyclone number concentration for a narrow size range of particles. The concentration in a narrow range was measured by the APS for 52 size channels between 0.5–20 μm . Each APS measurement was based on 10 scans with 20 seconds per scan. To account for small fluctuations in number concentration, the average was taken of pre-cyclone measurements made immediately before and after the post-cyclone measurement. (This led to the following series of measurements: pre—post

(1)—pre—post (2)—pre—post (3)—pre.) Using the mean penetration efficiency measurement, cyclone performance was compared to the ICRP curve given by the International Standards Organization (ISO), Comité Européen de Normalization (CEN), and the American Conference of Governmental Industrial Hygienists (ACGIH). The conventional method for comparing penetration efficiency to a size-selection standard is through the use of bias maps and is described by the following:

Assuming workplace aerosols are unimodal with a lognormal distribution, they can be described by the mass median aerodynamic diameter (MMAD) and geometric standard deviation (GSD). For any combination of these two values, a difference in collection efficiency can be calculated for the tested cyclone and an ideal cyclone that performs exactly in accordance with the size-selection standard. A plot of bias for all points in a space bounded by reasonable ranges of MMAD and GSD is called a bias map. The objective is to find the cyclone flow rate that most minimizes the ICRP bias rather than to best meet the diameter associated with 50% particle penetration ($_{50}d_{ae}$).

The estimated bias was calculated using Equations 1–3.^{42–44} A lognormal distribution was assumed and the calculated ranges of the MMAD and GSD were 1–30 μm and 1.5–4, respectively. The bias of the sampler (Δ) is defined as:

$$\Delta = \frac{\bar{C} - C_{st}}{C_{st}}, \quad (1)$$

$$\bar{C} = \int_0^\infty \bar{E}(D)A(D)dD, \quad (2)$$

where \bar{C} is the mean measured concentration, $\bar{E}(D)$ is the mean sampling efficiency of the sampler, and $A(D)$ is the normalized size distribution.

$$C_{st} = \int_0^\infty \bar{F}(D)A(D)dD, \quad (3)$$

where C_{st} is the ideal concentration, $\bar{F}(D)$ is the sampling efficiency of an ideal sampler, which perfectly follows the desired sampling convention. Using Equations 1–3, the cyclone penetration efficiency was compared to the ICRP over relevant MMAD and GSD.

The uncertainty due to the bias was determined using criteria of CEN Standard EN 13205:2014 and was calculated using following equation:⁴⁵

$$\mu_{bias} = \sqrt{\left[\frac{1}{N_{SD}} \sum_1^{N_{SD}} \left(\frac{\bar{C} - C_{st}}{C_{st}} \right)^2 \right]}, \quad (4)$$

where N_{sd} is the number of relevant size distributions (i.e. 216) for workplace aerosols given by EN 13205:2014 (discretized unshaded area in Figure 4). Samplers that effectively follow the ICRP have bias values in the range of 0.05 – 0.10, while those that diverge from the ICRP have bias values near 0.20 – 0.25.⁴⁵

Segregator evaluation by the APS and CCSEM

The segregator was evaluated using the APS and CCSEM to determine the particle size distributions of the segregated samples. The APS measured the particle size distribution and concentration fluctuation during the segregation process. The concentration fluctuated because the dust feed rate varied at the SSPD inlet due to the non-uniform dust distribution on the sample platform, which is inherent to the SSPD design. The APS was mounted within the segregator (Figure 2) and particles were sampled isokinetically (Section, “Cyclone flow rate selection”) for particle size distribution measurements.

The particle size distribution of collected samples was analyzed by CCSEM (PSEM eXpressTM, ASPEX, PA). The CCSEM provides an automated measurement process for particle sizing and counting by way of a backscattered electron detector (BSED).^{46–49} The BSED contrast results from atomic number differences

in the particle sample (mineral dust) and the background substrate (carbonaceous filter).

Dust collected on the 70-mm filter (Figure 1) was prepared for CCSEM analysis. First, the dust cake was removed from the filter with a spatula. Subsequently, dust samples were prepared in a dilute slurry in isopropanol and de-agglomerated in an ultrasonic bath for 1 hour. The slurry was agitated by a vortex mixer while being pipetted onto the polycarbonate filter. The sample was mounted in a glass filter holder and vacuum filtered. Filter samples were placed on aluminum stubs with conductive carbon tape and sputter-coated with a thin gold film (Desk V, Denton Vacuum, NJ). Particles were analyzed at $2.5\text{--}7.5 \times 10^3$ times magnification and 20 keV to determine projected area diameter and aspect ratio. About $3\text{--}5 \times 10^3$ particles were analyzed for each sample.

CCSEM measurements of projected area diameter were expressed in terms of aerodynamic diameter. Aerodynamic diameter was estimated from projected area diameter by accounting for morphology effects through the volume shape factor and dynamic shape factor. The volume shape factor (k_v) was calculated using a general expression that includes aspect ratio as a variable:⁵⁰

$$k_v m_a \sqrt{n_a} = k_e \quad (5)$$

where n_a is the elongation aspect ratio, m_a is the flakiness aspect ratio, and k_e is a value that depends on particle angularity. A value of 0.43 was used as an intermediate k_e for particles between tetrahedral and smooth shapes⁵⁰ and the aspect ratio for flakiness was assumed to be 1. The measured aspect ratios for elongation were 1.58 for calcite and 1.63 dolomite. Using the above values in Equation 5, the volume shape factors were 0.34 for calcite and dolomite.

Dynamic shape factors were determined previously for calcite and dolomite and were found to be 1.05 and 0.97, respectively.⁵¹ With the above shape factors, aerodynamic diameters (d_{ae}) were determined using the following expression (adapted from Wagner and Leith, 2001):⁵²

$$d_{ae} = d_{pa} \left(\frac{\rho_p}{\rho_0 \chi} \right)^{\frac{1}{2}} \left(\frac{\pi}{6 k_v} \right)^{\frac{1}{3}} \left(\frac{C_{c,dve}}{C_{c,dae}} \right) \quad (6)$$

where ρ_0 is unit density by definition of d_{ae} , ρ_p is the material density of 2.71 for calcite and 2.87 g/cm^3 for dolomite, χ is the dynamic shape factor, and $C_{c,dve}$ and $C_{c,dae}$ are slip correction factors for volume-equivalent diameter (d_{ve}) and aerodynamic diameter, respectively. $C_{c,dve}$ and $C_{c,dae}$ were approximated with a value of 1 because particle diameters were much

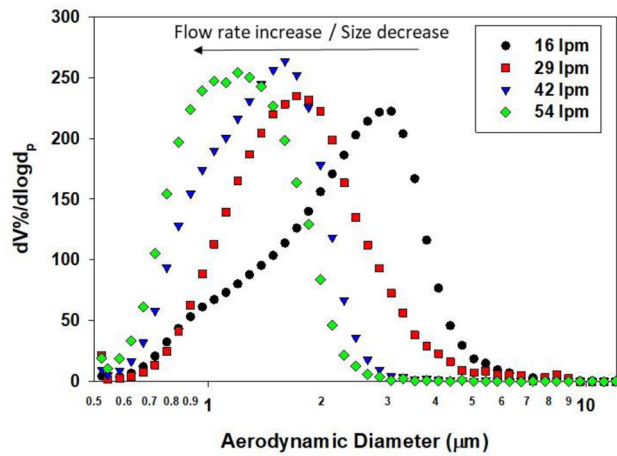


Figure 3. Aerodynamic particle size measurements of the particle size distribution measured downstream of the cyclone as shown in Figure 2.

larger than the air mean free path.⁵³ The conversion of CCSEM measurements to aerodynamic diameters using Equation 6 allowed reporting data with the same metric as APS measurements and ICRP criteria.

Results and discussion

Cyclone flow rate

The cyclone was calibrated for respirable dust separation by measuring the particle size distribution downstream of the cyclone for several flow rates (Figure 2). The lowest value tested (nominal value 16 lpm and actual value 16.3 ± 0.2 lpm) was limited by the requirement of a sufficient flow rate for particle de-agglomeration in the SSPD.⁵⁴ The highest value tested (54 lpm) was limited by the ability to maintain the flow rate despite an increasing pressure drop across the filter during particle collection. The comparison of the size distributions in Figure 3 shows that a flow rate of 16 lpm enabled adequate respirable dust separation and allowed for the inclusion of 2–4 μm particles, while larger flow rates exclude much of the 2–4 μm size range. The flow rate of 16 lpm was selected so that 2–4 μm particles were included in the respirable dust sample in an effort to follow ICRP criteria.

Cyclone performance

The ability of the cyclone to approximate the ICRP was evaluated by determining the difference in collection efficiency for the tested cyclone and an ideal sampler that performs in accordance with ICRP through the bias (Equations 1–3). The overall goal was to determine the uncertainty due to the bias

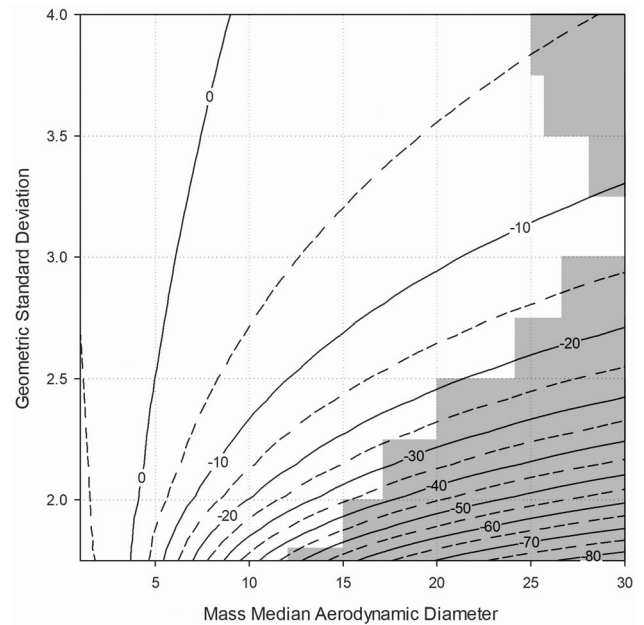


Figure 4. Bias map obtained using cyclone penetration efficiency measurements made in an aerosol chamber and calculations based on Equations 1–3. The unshaded area represents particle sizes most relevant to workplace aerosol exposures (EN 13205-2:2014).

(Equation 4) that resulted from the calibration of the cyclone at a flow rate of (16.3 ± 0.2) lpm. The evaluation of the bias map (Figure 4) showed that bias values were within $\pm 10\%$ for sub-5 μm particles but increased for larger MMAD. The increase for larger particles occurred because the cyclone had a sharper cut than the ICRP. The sharp cut provides a more uniform sample, which helps to establish consistent dose-response curves in health effects studies, while the divergence from the ICRP was not appreciable. The uncertainty due to the bias of the collected sample was 0.10 according to EN 13205:2014 criteria. These results suggest that size selection by the segregator effectively followed the ICRP. Similar to other evaluators of respirable samplers, it was assumed that the penetration curve is almost zero for particles larger than 10–15 μm . This assumption is supported by the lack of super-10 μm particles in aerosol size distributions measured within the segregator (Figure 2) since these particles were in the bulk dust (Figure 7), were suspended by the SSPD, and were most likely airborne at the cyclone inlet.

Although the bias is the primary indicator of performance, the evaluation of 50% cutoff diameter is useful for comparison with the ICRP recommendation and conventional cyclones. The 50% cutoff diameter was determined from pre-cyclone and post-cyclone particle size distribution measurements made in an aerosol chamber (Figure 5) to determine the sampling

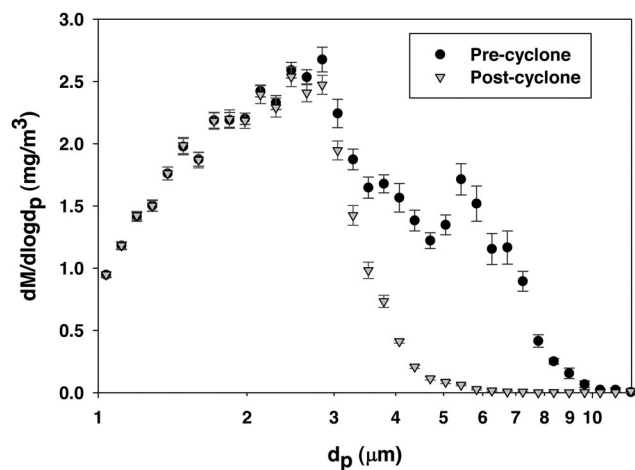


Figure 5. Pre-cyclone and post-cyclone particle mass-size distribution measurements made in an aerosol chamber to characterize penetration efficiency.

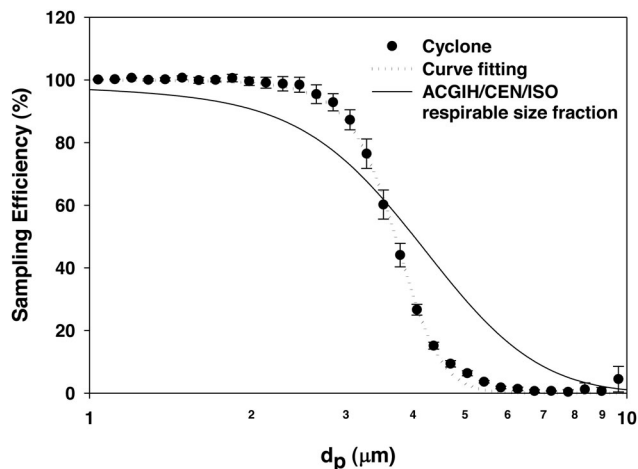


Figure 6. Sampling efficiency (or penetration efficiency) of the cyclone (filled circles), its fitted curve (dotted line), and the criteria given by the international (ACGIH/CEN/ISO) convention for respirable particles (solid line).

efficiency (or penetration efficiency) as a function of particle size. The sampling efficiency was plotted alongside ICRP criteria in Figure 6 and indicated a $_{50}d_{ae}$ of $(3.7 \pm 0.1) \mu\text{m}$ at (16.3 ± 0.2) lpm for the current cyclone. In comparison, a $_{50}d_{ae}$ of $(3.8 \pm 0.1) \mu\text{m}$ at (1.7 ± 0.1) lpm was measured for a conventional respirable dust cyclone (Dorr-Oliver) using the same aerosol chamber system. The comparison suggests that the current cyclone and conventional cyclone had similar cutoff diameters and that both were near the ICRP recommendation.

Segregator evaluation

Following the calibration, the cyclone was evaluated within the segregator system. This was done using the

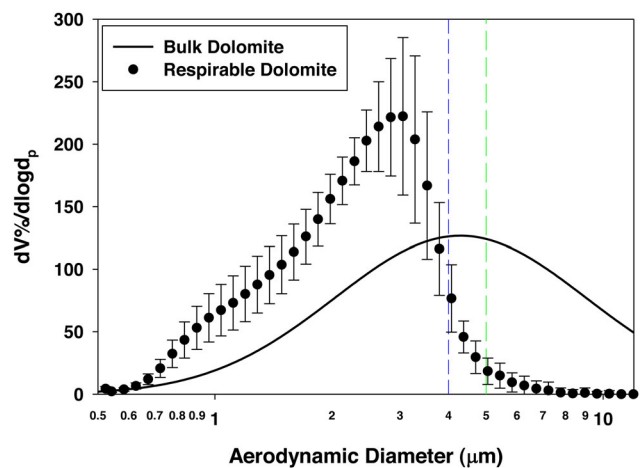


Figure 7. Comparison of the bulk (solid line) and respirable (filled circles) volume-size distributions for dolomite. The error bars reflect the fluctuation in particle concentration from the variation in bulk dust concentration at the SSPD inlet due to its inherent design. Despite the fluctuation, the concentration of super-4- μm particles remained low, in consistency with the ICRP.

APS to measure the particle size distribution downstream of the cyclone (Section, “Cyclone flow rate selection”, Figure 2). The evaluation by the APS showed that the segregator produced respirable size range particles as indicated by the comparison of the bulk dust size distribution and the respirable dust size distribution for dolomite in Figure 7. The comparison shows that the segregator reduced the super-4- μm range and retained the sub-4- μm range in consistency with the ICRP. The fluctuation of the particle concentration (indicated by the error bars) reflects the fluctuation of the inlet dust concentration due to the inherent design of the dust disperser. (The disperser samples dust from a rotating platform with a variable mass on the surface.) Despite this fluctuation, the concentration of super-4- μm particles remained low. Consequently, the variability of the bulk dust concentration at the inlet was not problematic for the segregator.

In addition, the segregator was evaluated by CCSEM to determine the particle size distribution of dust collected on the 70-mm filter, which is shown Figure 1. A sintered metal filter was employed for dust collection because of its durability, but if a biologically inert material is required, Teflon filters of the design—Fluoropore (Model FMLW, Millipore Sigma, MA)—were suitable for dust collection and removal. Suitability for removal was determined by measuring the mass loss of a blank filter after scraping the surface with a spatula. The blank filters were weighed in a temperature- and humidity-controlled chamber using a microbalance with 0.1- μg resolution and a

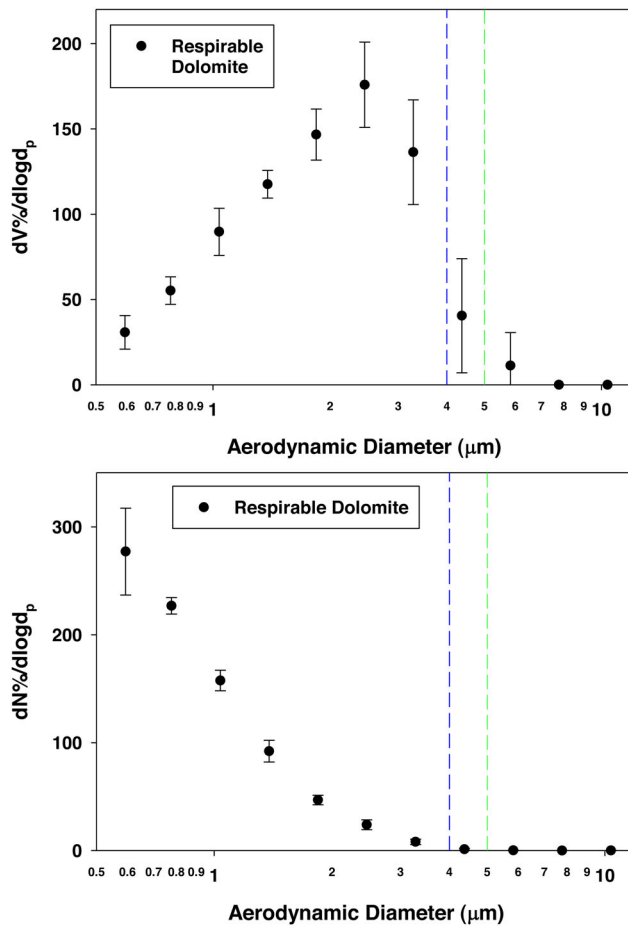


Figure 8. Particle volume-size and number-size distributions for segregated dolomite dust collected on the 70-mm filter as measured by CCSEM for thousands of particles per trial.

static neutralizer with a Po-210 source. The filter mass remained the same after scraping the entire surface with the edge of a metal spatula (average mass loss $0.2 \mu\text{g} \pm 1.0 \mu\text{g}$), and therefore the filter should not give off material to the respirable dust sample.

The CCSEM measurements confirmed APS results for non-caking dust and demonstrated robustness for caking dust as shown by the respirable dust volume-size distributions and number-size distributions in Figures 8 and 9. Particles larger than the respirable size range were infrequent and were attributed to particle bounce in the cyclone. The frequency was about 1 per 3,500 particles for dolomite and 1 per 5,000 particles for calcite (Table 1). The presence of these particles may be reduced by the addition of an elutriator before cyclone, and the addition is suggested for a future study.

Respirable dust yield

The segregator enabled the collection of a substantial mass of respirable dust. The respirable dust yield was

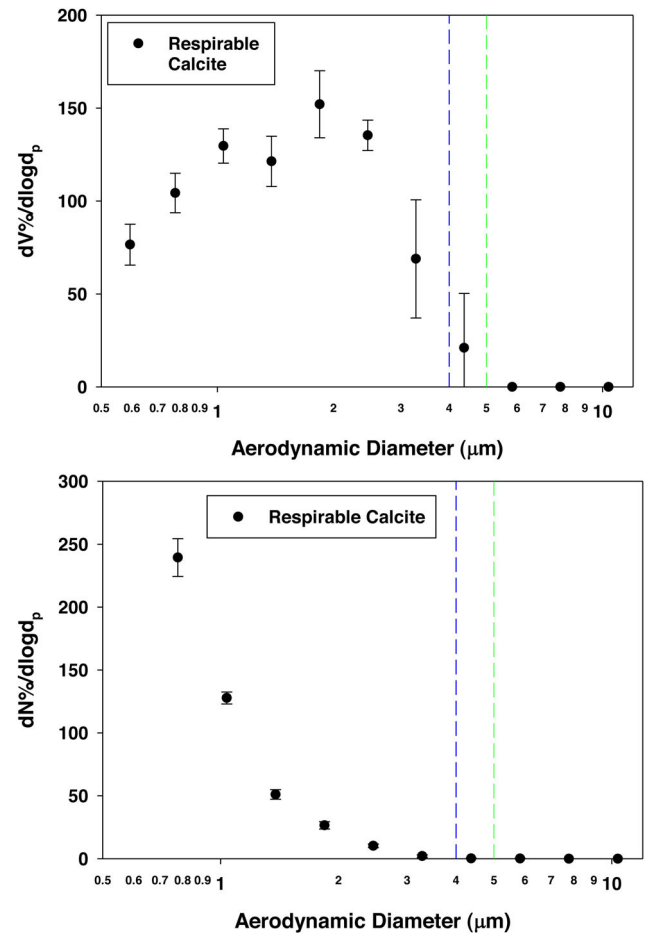


Figure 9. Particle volume-size and number-size distributions for segregated calcite dust collected on the 70-mm filter as measured by CCSEM for thousands of particles per trial.

Table 1. Estimation of particle bounce based on CCSEM analysis.

Dust Analyzed by CCSEM	Total Number of Particles Analyzed	Frequency of Particles Attributed to Bounce
Respirable Dolomite	14,305	1 per 3,500
Respirable Calcite	24,236	1 per 5,000

50 mg/hr for non-hygroscopic samples of dolomite and 30 mg/hr for hygroscopic samples of calcite. The yield for other samples will depend on the initial size distribution of the bulk dust. Bulk dust produced by high-energy processes often has an appreciable respirable dust content, and its segregation can lead to greater yields than observed in the current study. However, using the current samples for a conservative estimate, respirable dust can be amassed for chemical and toxicological evaluations in two working days or less. Specifically, 10 hours of operation would provide a batch of 500 mg of non-caking dust. A batch of 500 mg is referenced because it allows for a set of analyses, such as characterization by inductively coupled plasma mass spectrometry and *in vitro* toxicological assays, as indicated by Veranth and colleagues.²⁵ The current

segregator enabled the collection of substantial masses according to the ICRP, such that routine sample preparation is feasible for systematic health effects studies.

Alternatively, several conventional samplers may be placed in an aerosol chamber to amass respirable dust. However, conventional sampler performance often degrades as large masses (order of tens of milligrams) are collected. The cause depends on the sampler type, and for personal samplers with a cyclone, the cyclone flow rate decreases due to the high pressure drop across the dust-laden filter. In impactors, particle bounce becomes frequent as the impaction plate is laden with dust, and for foam filters, the sampling efficiency for respirable dust changes as coarse dust is collected. These effects lead to divergence from the ICRP and were avoided by using the current segregator.

The segregator can be thoroughly purged to prevent cross-contamination of samples by disassembling and sonicating. In addition, purging the reservoir for discarded dust (cyclone grit pot) should be done to prevent re-entrainment of discarded particles into the respirable dust sample. The cyclone grit pot was emptied every 2 hours for the horizontal cyclone configuration (Figure 1). If a vertical orientation is used, the grit pot can be emptied less frequently because the settled powder does not approach the top of the grit pot as quickly. Use of vertical orientation is a viable option because it did not affect size-separation performance.

The segregator was used to isolate the respirable fraction of bulk dust. It can also be employed to generate surrogates for industrial or atmospheric dust. Surrogates allow for the evaluation of respirable dust property effects on analytical method performance. To generate surrogates for method evaluations, bulk dust of pure minerals can be segregated to generate pure respirable minerals. Subsequently, accurate masses of respirable minerals can be mixed to simulate industrial or atmospheric respirable dust. This would allow for the evaluation of real-world mixture effects on analytical method performance. For example, mixing accurate amounts of respirable dust allows the investigation of mixture composition effects on RCS quantification by Fourier transform infrared spectroscopy.

Conclusions

A dust segregator was developed to approximate size-separation criteria of the international convention for respirable particles. Because the system allows for the segregation of substantial masses of respirable dust (e.g. 500 mg) in a relatively short time (e.g. 2 working days or less), it improves the feasibility of health

effects studies. It also makes the generation of respirable dust mixtures for analytical method development and assessment a routine task. The dust segregator consisted of a modified small-scale dust disperser, sharp-cut cyclone, and 70-mm filter that can be thoroughly purged to prevent cross-contamination of samples. The uncertainty due the sample collection bias was 0.10 according to EN 13205:2014 criteria, which suggests that cyclone performance effectively followed the convention. In addition, the 50% cutoff diameter ($3.7 \pm 0.1 \mu\text{m}$) approximated the convention recommendation of $4 \mu\text{m}$ and that of a personal exposure cyclone (Dorr-Oliver) ($3.8 \pm 0.1 \mu\text{m}$). Respirable dust size distributions were confirmed by aerodynamic particle sizer and computer-controlled scanning electron microscopy measurements for airborne particles penetrating the cyclone and for particles collected on the 70-mm filter, respectively. The segregator generated 50 mg/hr of non-caking respirable dust of dolomite and 30 mg/hr of caking respirable dust of calcite. The frequency estimated for particle bounce was 1 per 3,500 particles for dolomite and 1 per 5,000 particles for calcite. The reduction of particle bounce in the segregator may be considered for a future study.

Notes

The findings and conclusions in this paper are those of the authors and do not necessarily represent the official position of the National Institute for Occupational Safety and Health, Centers for Disease Control and Prevention. Mention of any company or product does not constitute endorsement by NIOSH.

Acknowledgements

The authors thank Andrew Cecala of NIOSH for discussions on respirable dust sampling.

Disclosure statement

There are no conflicts to declare.

ORCID

Boris Mizaikoff  <http://orcid.org/0000-0002-5583-7962>

References

1. Laney AS, Weissman DN. Respiratory diseases caused by coal mine dust. *J Occup Environ Med*. 2014;56:S18.
2. Santo Tomas LH. Emphysema and chronic obstructive pulmonary disease in coal miners. *Curr Opin*

- Pulm Med.* 2011;17(2):123–125. doi:10.1097/MCP.0b013e3283431674.
3. Schenker MB, Pinkerton KE, Mitchell D, et al. Pneumoconiosis from Agricultural Dust Exposure among Young California Farmworkers. *Environ Health Perspect.* 2009;117(6):988–994. doi:10.1289/ehp.0800144.
4. Linch KD. Respirable concrete dust-silicosis hazard in the construction industry. *Appl Occup Environ Hyg.* 2002;17(3):209–221. doi:10.1080/104732202753438298.
5. Crooks JL, Cascio WE, Percy MS, et al. The association between dust storms and daily non-accidental mortality in the United States, 1993–2005. *Environ Health Perspect.* 2016;124(11):1735–1743. doi:10.1289/EHP216.
6. Vodonos A, Friger M, Katra I, et al. The impact of desert dust exposures on hospitalizations due to exacerbation of chronic obstructive pulmonary disease. *Air Qual Atmos Health.* 2014;7(4):433–439. doi:10.1007/s11869-014-0253-z.
7. Johnston F, Hanigan I, Henderson S, et al. Extreme air pollution events from bushfires and dust storms and their association with mortality in Sydney, Australia 1994–2007. *Environ Res.* 2011;111(6):811–816. doi:10.1016/j.envres.2011.05.007.
8. Duffin R, Tran L, Brown D, et al. Proinflammatory effects of low-toxicity and metal nanoparticles in vivo and in vitro: highlighting the role of particle surface area and surface reactivity. *Inhal Toxicol.* 2007;19(10):849–856. doi:10.1080/08958370701479323.
9. Tran CL, Buchanan D, Cullen RT, et al. Inhalation of poorly soluble particles. II. Influence Of particle surface area on inflammation and clearance. *Inhal Toxicol.* 2000;12(12):1113–1126. doi:10.1080/08958370050166796.
10. Lison D, Lardot C, Huaux F, et al. Influence of particle surface area on the toxicity of insoluble manganese dioxide dusts. *Arch Toxicol.* 1997;71(12):725–729. doi:10.1007/s002040050453.
11. Lippmann M. “Respirable” dust sampling. *Am Ind Hyg Assoc J.* 1970;31(2):138–159. doi:10.1080/0002889708506223.
12. Miller BG, MacCalman L. Cause-specific mortality in British coal workers and exposure to respirable dust and quartz. *Occup Environ Med.* 2010;67(4):270–276. doi:10.1136/oem.2009.046151.
13. Soutar CA, Miller BG, Gregg N, et al. Assessment of human risks from exposure to low toxicity occupational dusts. *Ann Occup Hyg.* 1997;41(2):123–133. doi:10.1016/S0003-4878(96)00014-2.
14. Cherrie JW, Brosseau LM, Hay A, et al. Low-toxicity dusts: current exposure guidelines are not sufficiently protective. *Ann Occup Hyg.* 2013;57(6):685–691. doi:10.1093/annhyg/met038.
15. Calvert GM, Rice FL, Boiano JM, et al. Occupational silica exposure and risk of various diseases: an analysis using death certificates from 27 states of the United States. *Occup Environ Med.* 2003;60(2):122–129. doi:10.1136/oem.60.2.122.
16. Donaldson K, Seaton A. A short history of the toxicology of inhaled particles. *Part Fibre Toxicol.* 2012;9:13. doi:10.1186/1743-8977-9-13.
17. Cook AG, Weinstein P, Centeno JA. Health effects of natural dust. *Biol Trace Elem Res.* 2005;103:1–15.
18. Leung CC, Yu IT, Chen W. Silicosis. *Lancet.* 2012;379(9830):2008–2018. doi:10.1016/S0140-6736(12)60235-9.
19. Pavan C, Fubini B. Unveiling the variability of “Quartz Hazard” in light of recent toxicological findings. *Chem Res Toxicol.* 2017;30(1):469–485. doi:10.1021/acs.chemrestox.6b00409.
20. Warheit DB, Webb TR, Colvin VL, et al. Pulmonary bioassay studies with nanoscale and fine-quartz particles in rats: toxicity is not dependent upon particle size but on surface characteristics. *Toxicol Sci.* 2007;95(1):270–280. doi:10.1093/toxsci/kfl128.
21. Donaldson KE, Borm PJ. The quartz hazard: a variable entity. *Ann Occup Hyg.* 1998;42(5):287–294. doi:10.1016/S0003-4878(98)00044-1.
22. IARC Monograph. *IARC Monograph on the Evaluation of the Carcinogenic Risk of Chemicals to Humans Vol. 68: Silica, Some Silicates, Coal Dust and Para-Aramid Fibrils.* Geneva: IARC Press; 1997.
23. Clouter A, Brown D, Höhr D, et al. Inflammatory effects of respirable quartz collected in workplaces versus standard DQ12 quartz: particle surface correlates. *Toxicol Sci.* 2001;63(1):90–98. doi:10.1093/toxsci/63.1.90.
24. Volckens J, O’Shaughnessy PT, Hemenway DR. An aerosol generation system for the production of respirable grain dust. *Appl Occup Environ Hyg.* 1998;13(2):122–126. doi:10.1080/1047322X.1998.10389136.
25. Veranth JM, Smith KR, Aust AE, et al. Coal fly ash and mineral dust for toxicology and particle characterization studies: equipment and methods for PM2.5- and PM1-enriched samples. *Aerosol Sci Technol.* 2000;32(2):127–141. doi:10.1080/027868200303830.
26. Lam CW, James JT, McCluskey R, et al. Pulmonary toxicity of simulated lunar and martian dusts in mice: I. Histopathology 7 and 90 Days After Intratracheal Instillation. *Inhal Toxicol.* 2002;14(9):901–916. doi:10.1080/08958370290084683.
27. Teague SV, Veranth JM, Aust AE, et al. Dust generator for inhalation studies with limited amounts of archived particulate matter. *Aerosol Sci Technol.* 2005;39(2):85–91. doi:10.1080/027868290903899.
28. Liu Y, Schnare DW, Eimer BC, et al. Dry separation of respirable lunar dust: providing samples for the lunar airborne dust toxicity advisory group. *Planet Space Sci.* 2008;56(11):1517–1523. doi:10.1016/j.pss.2008.08.003.
29. Gonzales P, Felix O, Alexander C, et al. Laboratory dust generation and size-dependent characterization of metal and metalloid-contaminated mine tailings deposits. *J Hazard Mater.* 2014;280:619–626. doi:10.1016/j.jhazmat.2014.09.002.
30. International Organization for Standardization, ISO 7708:1995. Air quality—particle size fraction definitions for health-related sampling; 1995.
31. CEN, European Committee for Standardisation (CEN). Workplace atmospheres—size fraction definitions for measurement of airborne particles, CEN Standard EN 481; 1993.
32. ACGIH, American Conference of Governmental Industrial Hygienists (ACGIH). Threshold Limit

- Values (TLVs) and Biological Exposure Indices (BEIs). ACGIH; 2014.
33. Pensis I, Luetzenkirchen F, Friede B. SWeRF-A method for estimating the relevant fine particle fraction in bulk materials for classification and labelling purposes. *Ann Occup Hyg*. 2014;58(4):501–511. doi:10.1093/annhyg/met076.
34. Kuempel ED, Attfield MD, Vallyathan V, et al. Pulmonary inflammation and crystalline silica in respirable coal mine dust: Dose response. *J Biosci*. 2003;28(1):61–69. doi:10.1007/BF02970133.
35. Liebers V, Raulf-Heimsoth M, Brüning T. Health effects due to endotoxin inhalation (review). *Arch Toxicol*. 2008;82(4):203–210. doi:10.1007/s00204-008-0290-1.
36. Decker P, Cohen B, Butala JH, et al. Exposure to wood dust and heavy metals in workers using CCA pressure-treated wood. *J Am Ind Hyg Assoc*. 2002;63(2):166–171. doi:10.1202/0002-8894(2002)063<0166:ETWDAH>2.0.CO;2.
37. Hinds WC. *Aerosol Technology: Properties, Behavior, and Measurement of Airborne Particles*. New Jersey: John Wiley & Sons; 1999.
38. Gudmundsson A, Lidén G. Determination of cyclone model variability using a time-of-flight instrument. *Aerosol Sci Technol* 1998;28(3):197–214. doi:10.1080/02786829808965521.
39. Maynard AD, Kenny LC. Performance assessment of three personal cyclone models, using an Aerodynamic Particle Sizer. *J Aerosol Sci*. 1995;26(4):671–684. doi:10.1016/0021-8502(94)00131-H.
40. Kenny LC, Lidén G. A technique for assessing size-selective dust samplers using the APS and polydisperse test aerosols. *J Aerosol Sci*. 1991;22(1):91–100. doi:10.1016/0021-8502(91)90095-Y.
41. Cauda E, Sheehan M, Gussman R, et al. An evaluation of sharp cut cyclones for sampling diesel particulate matter aerosol in the presence of respirable dust. *Ann Occup Hyg*. 2014;58(8):995–1005. doi:10.1093/annhyg/meu045.
42. Bartley DL, Chen CC, Song R, et al. Respirable aerosol sampler performance testing. *J Am Ind Hyg Assoc*. 1994;55(11):1036–1046. doi:10.1080/15428119491018303.
43. Kenny LC, Bartley DL. The performance evaluation of aerosol samplers tested with monodisperse aerosols. *J Aerosol Sci*. 1995;26(1):109–126. doi:10.1016/0021-8502(94)E0071-5.
44. Aitken RJ, Baldwin PEJ, Beaumont GC, et al. Aerosol inhalability in low air movement environments. *J Aerosol Sci*. 1999;30(5):613–626. doi:10.1016/S0021-8502(98)00762-9.
45. CEN, European Committee for Standardisation (CEN). Workplace exposure—Assessment of sampler performance for measurement of airborne particle concentrations part 2: laboratory performance test based on determination of sampling efficiency, CEN Standard EN 13205-2:2014, 2014.
46. Jaques PA, Hopke PK, Gao P. Quantitative Analysis of Unique Deposition Pattern of Submicron Fe₃O₄ Particles Using Computer-Controlled Scanning Electron Microscopy. *Aerosol Sci Technol*. 2012;46(8):905–912. doi:10.1080/02786826.2012.680985.
47. EPA, U.S. Environmental Protection Agency. Guidelines for the application of SEM/EDX analytical techniques to particulate matter samples. EPA/600/R-02/070, 2002.
48. Mamane Y, Willis R, Conner T. Evaluation of computer-controlled scanning electron microscopy applied to an ambient urban aerosol sample. *Aerosol Sci Technol*. 2001;34(1):97–107. doi:10.1080/02786820118842.
49. Hopke PK, Casuccio GS. *Scanning Electron Spectroscopy, in Receptor Modeling for Air Quality Management*. P.K. Hopke, ed. Amsterdam: Elsevier Science; 1991: 149–212.
50. Davies CN. Particle-fluid interaction. *J Aerosol Sci*. 1979;10(5):477–513. doi:10.1016/0021-8502(79)90006-5.
51. Hudson PK, Young MA, Kleiber PD, et al. Coupled infrared extinction spectra and size distribution measurements for several non-clay components of mineral dust aerosol (quartz, calcite, and dolomite). *Atmos Environ*. 2008;42(24):5991–5999. doi:10.1016/j.atmos-env.2008.03.046.
52. Wagner J, Leith D. Passive aerosol sampler. Part I: Principle of operation. *Aerosol Sci Technol*. 2001;34(2):186–192. doi:10.1080/027868201300034808.
53. Friedlander SK. *Smoke, Dust, and Haze: Fundamentals of Aerosol Dynamics*. New York: Oxford University Press; 2000.
54. Chen BT, Yeh HC, Fan BJ. Evaluation of the TSI small-scale powder disperser. *J Aerosol Sci*. 1995;26(8):1303–1313. doi:10.1016/0021-8502(96)80777-4.